

Original Research

# Investigation of the Impact of Myco-Synthesized Silver Nanoparticles Against Soil Borne *Fusarium oxysporum*: Ultrastructure Appraisal

Dalia M. Al-Agamy<sup>1</sup>, Ahmed Atef<sup>1</sup>, Abdulmohsen Hussen Alqhtani<sup>2</sup>,  
Ahmed Ali<sup>3</sup>, Mohammed Yosri<sup>1\*</sup>

<sup>1</sup>The Regional Center for Mycology and Biotechnology, Al-Azhar University, 11787, Nasr City, Cairo, Egypt

<sup>2</sup>Animal Production Department, Food and Agriculture Sciences College, King Saud University, Riyadh, Saudi Arabia

<sup>3</sup>Department of Animal and Veterinary Sciences, Clemson University, 29630, Clemson, South Carolina, United States of America

Received: 11 October 2024

Accepted: 5 March 2025

## Abstract

Fungal biogenic production of silver nanoparticles (AgNPs) is a promising trend due to their facile handling and high metal tolerance. Moreover, they release a lot of extracellular molecules, which help to keep the nanoparticles in a steady form. *Fusarium oxysporum* (*F. oxysporum*) has a prolonged life span in the soil. It is one of the main causes of agricultural plants wilting in several commercially significant crops. In this investigation, a fungus was isolated from Minyat Al Nasr in Egypt, identified by traditional and molecular procedures as *Penicillium expansum* (*P. expansum*), and deposited in the gene bank with a code of PQ084992. *P. expansum* produced silver nanoparticles, which could be seen by a change in color. It has a notable peak at 420 nm through testing by UV spectrophotometry. Nanoparticles have been examined by electron microscopy, revealing their size range as 40-80 nm. The characterization has been completed using XRD, EDX, and FTTR. The myco-synthesized silver nanoparticles had anti-*F. oxysporum* with an inhibition zone of 23.1±1.2 mm, and its MIC was 15.6±0.6 µg/mL. This anti-*F. oxysporum* is produced by altering the ultrastructure of *F. oxysporum* when using the produced wilt disease in plants. Nanoparticles in relation to amphotericin B. Silver nanoparticles were tested on Vero cells and showed minimal cytotoxicity with IC<sub>50</sub> = 165.0±2.6 µg/mL. These results suggest the potential of applying myco-synthesized silver nanoparticles against fungal pathogens.

**Keywords:** *Penicillium expansum*, *Fusarium oxysporum*, myco-synthesis, electron microscope

\*e-mail: mohammed.yosri@yhao.com

## Introduction

Specialists have expressed worries about plant pathogens becoming an immediate danger to human and animal health [1]. Animals, poultry, and plants may acquire the phytopathogen *Fusarium oxysporum* [2]. *F. oxysporum* is one of the plant pathogens. It is considered the world's fifth most significant fungal plant pathogen that causes the greatest financial damage [3]. About 106 identified formae speciales of the *F. oxysporum* species complex (FOSC) invade over 100 distinct hosts and cause vascular wilts [4]. Their characteristics include being soilborne, having a long lifespan, being resistant to treatment with chemicals, and having the ability to quickly change past host resistance [5, 6]. They lead to total plant mortality and crop loss as hemibiotrophic infections, in addition to revenue loss [7].

*F. oxysporum*, the primary cause of Fusarium wilt disease, seriously damages plants at every growth stage [8]. In El-Badari, Assiut Governorate, Egypt, pomegranate trees were found to be wilting due to *F. oxysporum* for the first time in Upper Egypt [9]. *F. oxysporum* infections have recently caused serious damage to all phases of plant development, resulting in injuries to tomato production in up to 67% of Egypt's total planted area [10]. The fact that spores can persist in living conditions for several years and that remnants of pesticides have a harmful impact on human health has rendered the conventional methods of controlling the disease, such as using antifungal agents and crop rotation, ineffective. Therefore, it is imperative to enhance novel and effective control methodologies [11].

The developing implications of nanotechnology provide the potential to overcome the challenges facing agriculture. Novel nanomaterials and technological applications have been made possible by the development of nanotechnology in a variety of disciplines, including managing pests [12], food storage and packaging [13], and synthesizing fertilizers and pesticides. Due to their nanoscale dimension, nanomaterials typically present the potential for developing nano-fertilizers (NFs) with bioavailable substances that have excellent absorption and intake competence in both ways, through foliar application or by adding to the soil. This is due to their tiny dimensions ranging from less than 100 nm and abundant surface-to-volume ratio. Nanomaterials' novel chemical, physical, and visual properties enable their development as biochemical and natural sensor devices with fast analyte detection [14-16].

The outstanding properties of silver nanoparticles (AgNPs) include size-dependent biological, psychological, and physical aspects; these nanoparticles have been extensively studied [17]. The thermodynamic properties of silver nanoparticles, such as their point of melting and molar heat of fusion, are directly correlated with their particle diameter [18]. The antimicrobial properties of silver nanoparticles synthesized by environmentally friendly techniques have drawn attention to their possible uses in disinfection and

antimicrobial protection [19, 20]. The safety and ecological impacts associated with employing these nanoparticles must be taken into account to ensure their compatibility and reliability [21]. In this work, AgNPs were biosynthesized using isolated *Peculium expansum*, and their capacity to fight against *F. oxysporum*, which causes wilt disease, was investigated. AgNPs were also thoroughly characterized by TEM, FTIR, UV-vis, XRD, and EDX. Additionally, the ultrastructure alterations of *F. oxysporum* were examined.

## Materials and Methods

### Fungal Stain and Chemicals

*Fusarium oxysporum* (ATCC48112) was kindly provided by the Regional Center for Mycology and Biotechnology-Al-Azhar University. All chemicals used during this work were purchased from Sigma, Egypt.

### Collection of Specimens

Soil specimens were taken from various locations in Minyat Al Nasr in Egypt (31°07'34.46" N 31°38'35.27" E) following the excavation of 10-15 cm deep trenches. Prior to being utilized, the specimens were gathered and kept at 4°C in sterile zippered polythene bags [22].

### Isolation of Fungi

Various media were utilized, such as yeast extract, sucrose, potato dextrose, Czapek's dox, malt extract, and yeast malt extract agar medium. Techniques for isolation included the use of sprinkle plates. The soil was evenly distributed directly onto the medium's surface to create sprinkle plates. The plates were incubated at 25°C for 5-7 days. After being purified using the single spore and hyphal-tip procedure, the fungi growing on the agar plates were moved to malt extract slants, which were kept as a stock culture [23]. The ability of each isolate to produce AgNPs was examined and tested. The fungal isolate labeled was the sole isolate with a high production potential for AgNP biosynthesis (Fun 5).

### Identification of Fungi Using Standard and Molecular Methods

Based on its morphological characteristics and microscopic investigation, the isolated fungus with the greatest capacity to produce AGNPS was recognized at the genus and species level.

The fungal mycelium was macerated in Tris-EDTA buffer pH 7.9, which contained 1.6 M sodium chloride, 0.2 mg/mL proteinase K, 9.8 mM  $\beta$ -mercaptoethanol, and 2.0% SDS (w/v) in order to extract the DNA. A mixture of chloroform, isoamyl alcohol (23:1, v/v), and 3.0 M potassium acetate was used to purify the nucleic acids. After that, the DNA was separated using ethanol, dried at

ambient temperature, and rehydrated using DNase-free water. PCR was used to amplify the 18S rDNA. Primers A (5'-AACCTGGTTGATCCTGCCAGT-3') and 564R (3'GGCACCAGACTTGCCCTC-5') were used. The ABI 3730xl DNA sequencer (ThermoFisher, USA) was used to sequence the PCR results after being purified using a PCR purification kit. The BLAST (NCBI) search similarity analysis was utilized to compare the amplified product sequences. Using MEGA X, a phylogenetic tree was constructed using the neighbor-joining method to confirm the strain's phylogenetic area [24].

### Myco-Synthesis of AgNPs

Preparation involved putting the fungal Fun 5 into 200 mL of malt broth and mixing the mixture for 5 days (28±2) at 2000 rpm. The culture was spun for 20 minutes at 30100 xg after incubation to separate the pellet and supernatant. One milliliter (1 mM) of silver nitrate solution and 100 milliliters of supernatant were placed into a clean 250 milliliter conical flask. AgNO<sub>3</sub>-free control testing was conducted using the second reaction. To stop AgNO<sub>3</sub> from oxidizing, the mixture was left to stand in a dark, shaking incubator at 200 rpm and 37°C for a whole day. The yellow color of the cell-free extract changed to a brownish color with the addition of the precursor, allowing for visual verification of AgNPs formation. The supernatant was dried at 60°C and then crushed to produce a fine AgNP powder. AgNPs were carefully cleaned with distilled water to eliminate impurities from the control flask and then stored for characterization [25].

### Characterization of Myco-Synthesized AgNPs

Conventional characterization techniques, including ocular color change and a UV-visible spectrophotometer (Agilent UV-1200, USA), with a scanning spectra span of 300 to 700 nm were used. Transmission electron microscopy (JEOL 1010 TEM, Japan) investigated the morphology of AgNPs. X-ray diffraction (XRD) (Agilent 6000, USA) with a Cu-K $\alpha$  X-ray source ( $\lambda = 1.5418 \text{ \AA}$ ) analysis was used to assess the crystallite nature of AgNPs. Fourier transform infrared spectroscopy (FTIR) (Agilent, USA) was utilized to study the functional groups involved in reducing, capping, and stabilizing AgNPs. The standard operating protocol was followed in order to determine the spectral bands of prepared (crystallized form) AgNPs. An x-ray microanalysis (Oxford 6587, UK) linked to (JEOL, Japan) scanning microscopy for EDX testing [26].

### Antifungal Impact of Myco-Synthesized AgNPs

Agar well diffusion was used to assess AgNPs' effects on *F. oxysporum*. The fungus was cultured on PDA plates and kept at 28±2.0°C for 5 days. A suspension of 10<sup>7</sup> spores/mL of fungal suspension in a sterilized phosphate buffer solution pH 7.0 was

used. Agar MEA plates were evenly filled with one milliliter. Wells (8 mm) were cut using a sterile cork borer. 100  $\mu$ L of AgNPs and AgNO<sub>3</sub> were added to each well separately and incubated for two hours at 5°C. Following the application of a conventional antifungal, amphotericin B, the plates were incubated for five days at 28±2.0°C. The inhibitory zones were identified and noted following incubation. A serial level of AgNPs was tested to illustrate the minimal inhibitory level [27].

### Cytotoxicity Evaluation

Data was obtained from the American-type culture collection (ATCC), and the MTT technique was used to assess the cytotoxicity of AgNPs towards the Vero cell line [28].

### Transmission Microscopic Examination

In order to set up TEM samples, fungal specimens (about 1 mm, 3 each) were taken out of agar colonies. After being fixed in 3% glutaraldehyde and rinsed in phosphate buffer, the samples were post-fixed in potassium permanganate solution for five minutes at ambient temperature. The specimens were soaked in ethanol dilutions ranging from 10% to 90% for 15 minutes each, and then they were dried for 30 minutes in 100% ethanol. They were then injected with acetone and epoxy resin in a graduated sequence before being immersed in pure resin. Copper grids were used to capture extremely tiny particles. Uranyl acetate and lead citrate were then used three times to stain the sections. A 70 kV voltage was applied to the (JEOL 1010, Tokyo, Japan) transmission electron microscope to evaluate stained slices [29].

### Statistical Testing

All experiments were conducted three times, and GraphPad Prism V5 (CA, USA) was used to determine the means and standard errors.  $P < 0.05$  was used to represent a dramatic difference.

## Results and Discussion

### Fungal Isolation and Identification

The fungus in the petri dish had a pale green color, an axially sulcate appearance, a crocheted texture, and a yellow inverse yellow, according to the examination of the color change by the naked eye. However, a light microscope inspection revealed that it had branching septal conidiophores with sporulating cells and gloomy green, cylindrical conidia. The isolated fungus's whole macroscopic and microscopic analysis is available in (Fig. 1). The fungal identification was confirmed using 18s rRNA. The fungus was identified as *P. expansum*, and the phylogenetic tree was created and showed



Fig. 1. Microscopic examination of *P. expansum* (magnification = 40X). The fungus was terverticillate with smooth spta. Where conidiophores were 200-400  $\mu\text{m}$  long; Metula was 12  $\mu\text{m}$ ; phalides were 10  $\mu\text{m}$  long; and globose conidia were 2-4 X 2.3 -3.4  $\mu\text{m}$  in size.

an interconnected connection between it and other *Penicillium* spp., as shown in (Fig. 2). The sequencing information was submitted to the Gene Bank under the accession code PQ084992. (<https://www.ncbi.nlm.nih.gov/nucleotide/PQ084992>). The 18S rRNA sequences of

genes are the target of multiple primers unique to fungi and are a well-known marker for fungal categorization [30, 31]. This is in accordance with Park et al. [32], who followed the same steps for identifying isolated *Penicillium* species from different regions. Furthermore, Demjanová et al. [33] applied the same classical protocol for *Penicillium* sp. identification.

### Green Production of Silver Nanoparticles Using *P. Expansum*

It was noted that, prior to 3 days of incubation, the color changed to brown, and silver nitrate reacted with the *P. expansum* cell-free extract. The positively energized Ag ions contacted the electrostatically polarized hydroxyl groups of the bioactive molecules in the filtrate, reducing them to Ag<sup>0</sup> and ultimately giving AgNPs. No control color changes were made, as illustrated in (Fig. 3) in the same line as Mohammadi and Salouti [34], who followed the same steps to obtain silver nanoparticles from *Penicillium chrysogenum*. Furthermore, Ammar and El-Desouky [35] showed that *Aspergillus terreus* successfully produces AgNPs. Besides, Yassin et al. [36] illustrated that *Penicillium verrucosum* could be used to prepare silver nanoparticles.

### Characterizing the Prepared Silver Nanoparticles

#### UV Spectrophotometry

A UV-Vis spectrophotometry was applied to describe the prepared AgNPs in the initial phase, generating an absorbance peak at 420 nm (Fig. 4). A strong confined SPR was the trigger of the NPs stimulants. In accordance with earlier research, the form

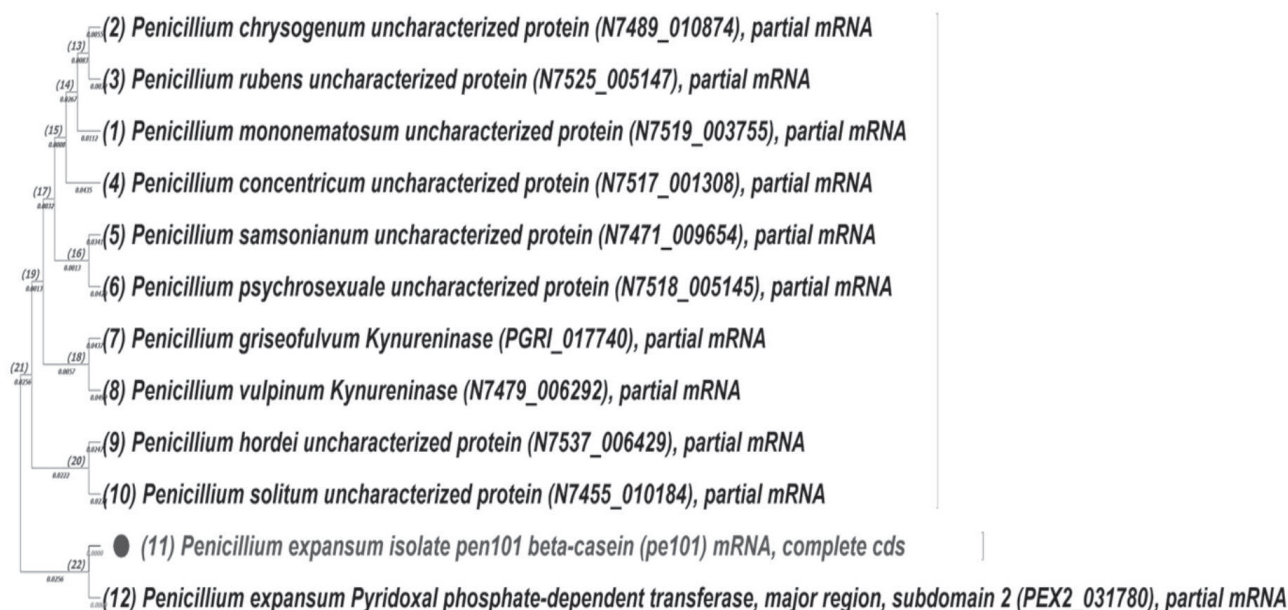


Fig. 2. Phylogenetic analysis of *P. expansum* by distance examination procedure of 18 s rRNA sequence of genes.





Fig. 3. Preparation of AgNPs using *P. expansum* (A) Cell-free extract of *P. expansum* (B) Color change after incubation of *P. expansum* cell-free extract with silver nitrate.

and dimensions of AgNPs are frequently associated with the particular SPR record [37]. This is in line with Guilger-Casagrande and Lima [38], who illustrated that the change of color upon the production of nanoparticles could be detected using a UV spectrophotometer. Additionally, Osorio-Echavarría et al. [39] showed that fungi could mediate the synthesis of silver nanoparticles and could be detected through color change and spectrophotometry. Moreover, Al-Soub et al. and Tang et al. [40, 41] showed that airborne fungi could produce silver nanoparticles at 420 nm.

#### Electron Microscopic Examination

Particles larger than 16.5 nm were visible in the TEM image; the size of the particles determined by TEM analysis differed from that determined using the Scherrer equation for XRD. The shift in active species, such as the amount of polyphenols in the cell-

free extract, may cause this. The speed of production and nucleation activities is slowed down when fewer species are active [42]. The dimensions, structure, and distribution of NPs are among the variables that affect their microbiological and physiological functions [43]. NPs' biocompatibility and effectiveness rose as their dimensions shrank [44]. As such, it is crucial to look at the structural characteristics of the NPs at TEM, which were represented as monodispersed circles with a size range of 40-80 nm. In accordance with Rudrappa et al. [45], *Penicillium brasilianum* could produce silver nanoparticles with a size of up to 60 nm. Meanwhile, Basheer et al. [46] used marine fungi to prepare AgNPs with dimensions of about 25 nm and showed that the TEM picture shows that monodispersed round AgNPs can be effectively reduced and capped by the culture extract's metabolites without aggregating (Fig. 5). TEM is better for the characterization of nanoparticles than TEM, as it has a simpler method for preparation, better resolution, and extra analytical tools [47].

#### EDX and XRD Analysis

EDX gives both quantitative and qualitative status to the components that could be associated with the production of AgNPs. The energy and amplitude pattern of X-ray impulses produced by a concentrated electron ray on a sample is measured as part of EDX testing. The findings are displayed in (Fig. 6a), which displays the profile from EDX spectra. It is evident through EDX examination that silver was present by 75% in the sample (Table 1). According to earlier research, silver nanoparticles exhibited peak absorbance at 3 keV [47]. In another investigation, it was revealed that AgNPs were bound by plant-based constituents via oxygen atoms as they were analyzed by EDX. The powerful signal of Ag atoms demonstrated the crystalline feature, and the existence of oxygen peaks

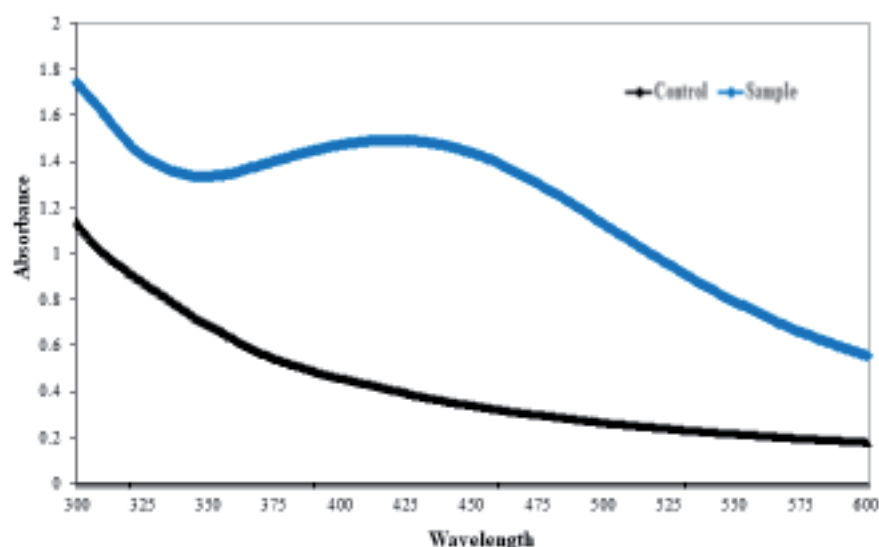


Fig. 4. UV-visible spectrophotometry for prepared AgNPs by *P. expansum* (blue peak); Cell-free extract of *P. expansum* (black line).

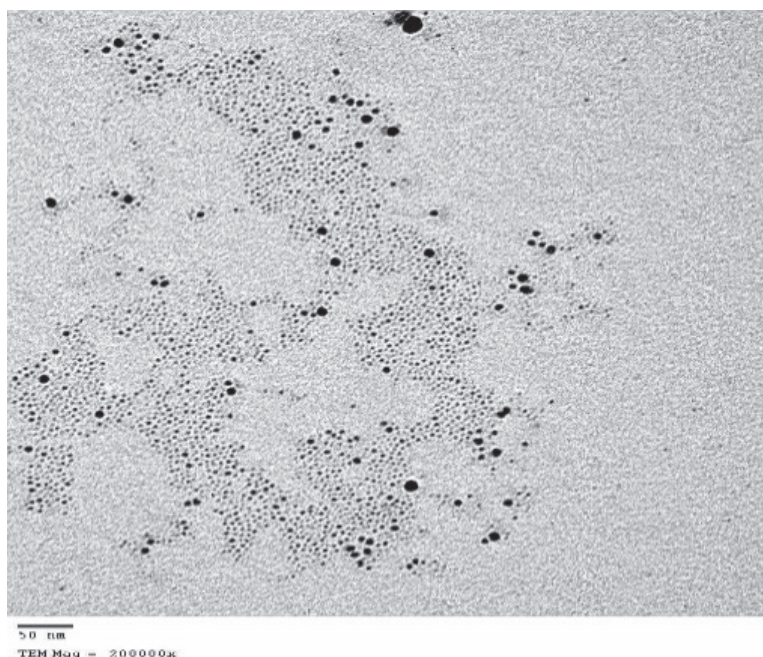


Fig. 5. TEM electron microscope micrograph showing different sizes of extracellular silver nanoparticles from *P. expansum* (x 200000).

together with the silver evidence demonstrated this [48, 49].

The XRD structure and the existence of peaks validate their production and illustrate the crystal form of prepared AgNPs. It showed the reflections in the range of 3-82° at  $2\theta = 31.14^\circ, 37.1^\circ, 47.2^\circ, 56.9^\circ, 63.1^\circ$ , and  $76.0^\circ$ , which match the XRD form of the planes (111), (200), (220), and (311), as shown in (Fig. 6b). Usually, the (111) surfaces of the crystal metallic silver nanoparticles are attributed to the peak at  $37.1^\circ$ . This suggests that the procedure yields AgNPs

with crystal forms of high grade. In accordance with earlier reports that illustrated similar forms of XRD [50, 36].

#### FTIR

The FTIR assessment of AgNPs (Fig. 7) showed intense peaks at 3442.8, 2923.32, 1634.86, 1367.62, 1219.45, 772.51, and  $673.13\text{ cm}^{-1}$ . The OH and the OH-extended group of phenols and alcohol or NH-extending of aliphatic primary amines could

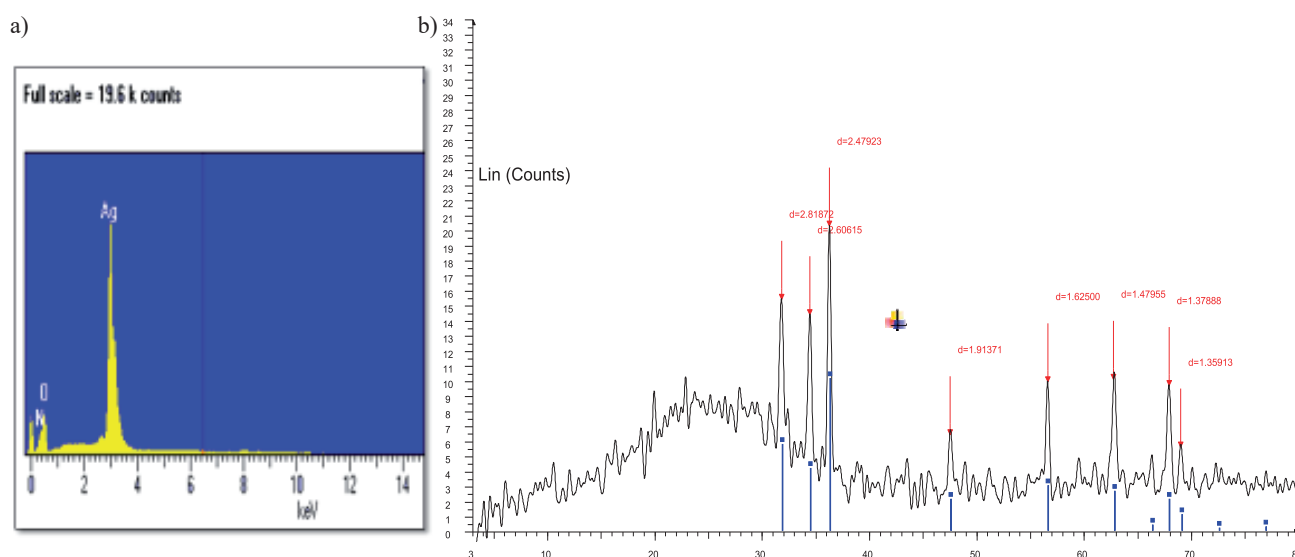


Fig. 6. a) X-ray microanalysis of AgNPs produced by *P. expansum* with a silver peak at 3KeV. b) XRD form of the prepared AgNPs by *P. expansum*.

Table 1. The percentage of elements produced by *P. expansum* after incubation with silver nitrate measured by X-ray micro-analyzer.

| Edx      | Elements Means of % $\pm$ standard deviation |    |    |
|----------|--|----|----|
| Elements | Ag   | O  | N  |
| %        | 75   | 13 | 12 |

potentially be responsible for the broad peak displayed at  $3442\text{ cm}^{-1}$  [51]. The peak at  $2923\text{ cm}^{-1}$  represented the C-H vibratory extending of aliphatic methyl ( $\text{CH}_3$ ). A mild migration of the amide-extending peak shifted from  $1640$  to  $1634\text{ cm}^{-1}$ . It could be linked to the charged connection among the exterior of AgNPs and the amide bonds of protein molecules, which was in agreement with the preceding research [52]. The observed peak at  $12190\text{ cm}^{-1}$  may result from C–O–C or C–O absorbance [53]. The expanding peaks at  $772$  and  $673\text{ cm}^{-1}$  were indicative of amides IV extended bends for proteins and alkenes ( $=\text{C-H}$  stretching) [54].

### Antifungal Impact

The present research assessed the antifungal capability of AgNPs towards *F. oxysporum* compared to amphotericin B. The results showed that, in comparison to the usual medication, the produced AgNPs demonstrated remarkable antifungal action against *F. oxysporum*, with inhibition zones of 23–25 mm consequently. Furthermore, the minimum inhibitory values (MICs) of silver nanoparticles versus *F. oxysporum* were ascertained and presented in

(Table 2). The MIC results indicated that the standard medication inhibited growth at  $3.9\text{ }\mu\text{g/mL}$  towards *F. oxysporum*, whereas the silver nanoparticles inhibited growth at values of  $15.6\text{ }\mu\text{g/mL}$ . Higher concentrations of AgNPs in solution may allow them to stick to and saturate fungus hyphae, killing the fungus cells.  $\text{Ag}^+$  is responsible for this inhibitory action, which mainly impacts the activity of membrane-associated proteins like those in the respiration pathway.  $\text{Ag}^+$  may also impact how some microbial protein and enzyme compounds are expressed. Documentation of DNA replication interruption has also been made. AgNPs may collaborate with precursors to inactivate enzymes and stop them from producing products necessary for cells' functioning via inhibitory competition [55, 28]. The most frequently used antifungal medication for treating fungal diseases is amphotericin B, which displays concentration-related fungicidal action towards the majority of fungal isolates (Borman et al., 2017). At a  $46\text{--}52\text{ }\mu\text{g/mL}$  dosage, AgNPs made from *P. chrysogenum* cell-free culture filtrates showed substantial antifungal effectiveness against the mycotoxigenic fungi [56]. AgNPs generated by *A. sydowii* were found to have antifungal action towards different species of *Aspergilli* by Wang et al. [57].

### Examination of The Role of Silver Nanoparticles Towards *F. Oxyspoum*

Ultra-thin examinations of normal cells of *F. oxyspoum* (Fig. 8a) showed cells with regular cytoplasm, homogenous cytoplasm, and a uniform pattern; the control cell's cell wall was completely incorporated and unharmed. There is a clear lysis in the cellular surface upon using the MIC of amphotericin

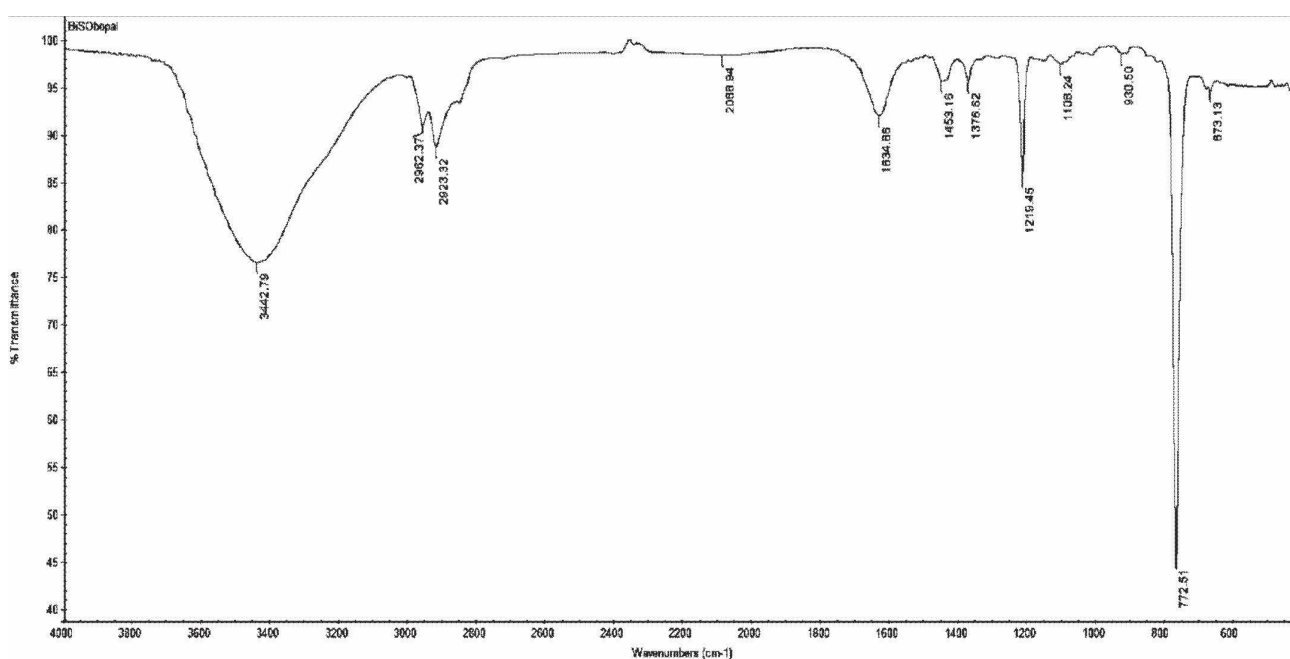


Fig. 7. FTIR pattern of AgNPs produced by *P. expansum*.



Table 2. Determination of the inhibition diameter (mm) and MIC ( $\mu\text{g/mL}$ ) for produced silver nanoparticles relative to the standard drug.

|                          | Silver nitrate | Silver nanoparticles | Amphotericin B |
|--------------------------|----------------|----------------------|----------------|
| Inhibition zone (mm)     | N.D            | 23.1 $\pm$ 1.2       | 25.0 $\pm$ 1.2 |
| MIC ( $\mu\text{g/mL}$ ) | N.D            | 15.6 $\pm$ 0.6       | 3.9 $\pm$ 0.2  |

B (Fig. 8b). Finally, applying the MIC of prepared silver nanoparticles leads to the alteration of cellular structure, including cellular surface and internal organelles, and the nanoparticles deposited in the outer surface lead to its antifungal impact and designation of fungal cells (Fig. 8(c, d)). This was in line with Akpınar et al. [58], who illustrated the fungicidal role of silver nanoparticles towards various *Fusarium* strains. Besides, Ansari et al. [59] explained the destruction of the fungal cells using electron microscopy examination.

### Impact of Myco-Prepared Silver Nanoparticles on The Cytotoxicity of Normal Cells

The MTT procedure was used to confirm the proportion of cell inhibition and assess the cytotoxic properties of biosynthesized AgNPs towards a Vero conventional cell line. (Fig. 9) shows the MTT in Vero cell lines subjected to AgNPs for 24 hours at various levels (15.62-1000  $\mu\text{g/mL}$ ). It could be noticed that the rise in AgNP level led to the decline in Vero cell survival. At 15.62  $\mu\text{g/mL}$  of AgNPs, 99.3% of the cells were still viable. At 1000  $\mu\text{g/mL}$  of AgNPs, however, cell viability was dramatically reduced to 10%, and the damaging percentage for Vero cells was 0.7% and 90% at 15.62 and 1000  $\mu\text{g/mL}$ , consecutively. The cytotoxic properties of these nanoparticles were indicated by the dramatic decrease in Vero cell lifespan that the AgNPs showed at an  $\text{IC}_{50}$  of 165.0 $\pm$ 2.6  $\mu\text{g/mL}$ . According to earlier research, the normal Vero cell demonstrated 100% viability at 15.63  $\mu\text{g/mL}$ , and survival dropped as the AgNP level increased with an  $\text{IC}_{50}$  of 279  $\mu\text{g/mL}$  [60-62]. In general, a substance is considered non-cytotoxic if its  $\text{IC}_{50}$  value is

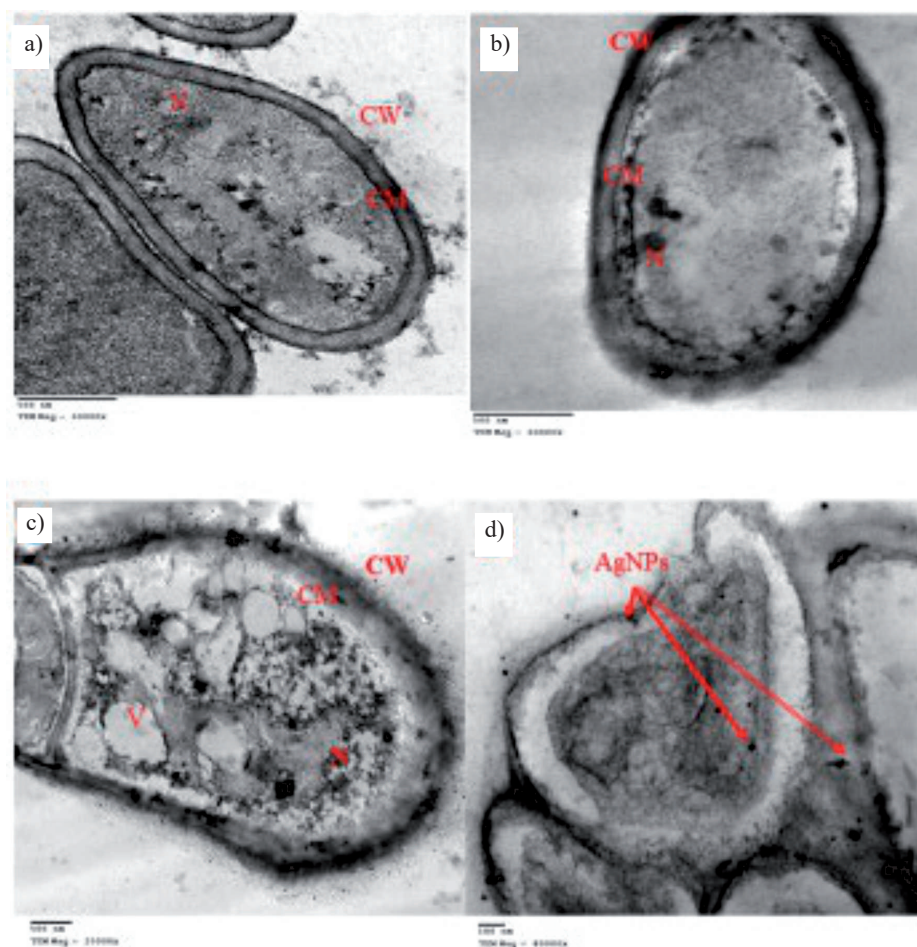


Fig. 8. TEM investigation of *F. oxyspoum* a) untreated cells (magnification = 4000X); b) Treated by amphotericin B; c) Treated by silver nanoparticles [Scale bar 500 nm] and d) Deposition of silver nanoparticles in the cellular surface of *F. oxyspoum* [Scale bar 100 nm].



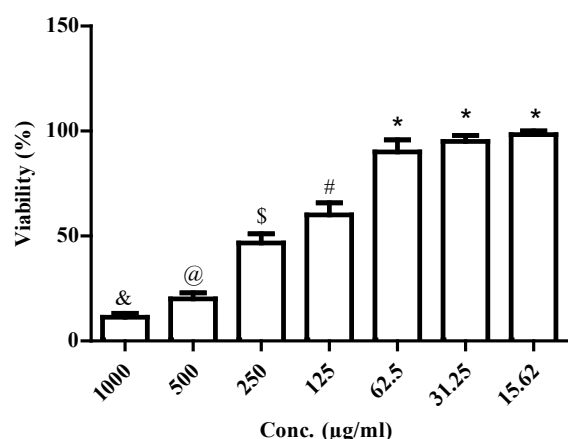


Fig. 9. Testing the cytotoxic impact of the myco-synthesized AgNPs towards the normal cell line ( $IC_{50} = 165.0 \pm 2.6$  µg/mL; various symbols refer to various levels of difference among levels).

greater than 90 µg/mL [57]. As a result, using the myco-synthesized AgNPs from this work is safe.

## Conclusion

The isolated *P. expansum* in this investigation could potentially be used to myco-synthesize silver nanoparticles. Their color could be seen by the naked eye and characterized by several instruments, including a UV-visible spectrophotometer, electron microscopy, FTIR, XRD, and FTIR. These nanoparticles have an antifungal impact on *F. oxysporum*, and this impact was confirmed using a transmission electron microscope, which illustrates the deposition of AgNPs in the fungal cells to be applied with high security towards normal cell lines. This could have an economic impact as it could be applied safely versus *F. oxysporum*, which could lead to many biohazards in crops and poultry infections.

## Conflict of Interest

The author confirms that they have no conflict of interest.

## Acknowledgments

This work was supported by Research Supporting Project, King Saud University, Riyadh, Saudi Arabia [grant number RSP-2025R439].

## References

1. EDEL-HERMANN V., LECOMTE C. Current status of *Fusarium oxysporum* formae speciales and races. *Phytopathology*, **109** (512), 2019.

2. NAG P., PAUL S., SHRITI S., DAS S. Defense response in plants and animals against a common fungal pathogen, *Fusarium oxysporum*. *Current Research Microbiology Science*, **3** (100135), 2022.
3. DEAN R., VAN KAN J.A., PRETORIUS Z.A., HAMMOND-KOSACK K.E., DI PIETRO A., SPANU P.D., RUDD J.J., DICKMAN M., KAHMANN R., ELLIS J. The Top 10 fungal pathogens in molecular plant pathology. *Molecular Plant Pathology*, **13** (414), 2012.
4. HUDSON O., FULTON J.C., DONG A.K., DUFAULT N.S., ALI M.E. *Fusarium oxysporum* f. sp. niveum Molecular Diagnostics Past, Present and Future. *International Journal of Molecular Science*, **22** (18), 9735, 2021.
5. PENG H., SIVASITHAMPARAM K., TURNER D. Chlamydospore germination and *Fusarium* wilt of banana plantlets in suppressive and conducive soils are affected by physical and chemical factors. *Soil Biology and Biochemistry*, **31** (1363), 1999.
6. AKHTER A., HAGE-AHMED K., SOJA G., STEINKELLNER S. Potential of *Fusarium* wilt-inducing chlamydospores, in vitro behaviour in root exudates and physiology of tomato in biochar and compost amended soil. *Plant Soil*, **406** (425), 2016.
7. LYONS R., STILLER J., POWELL J., RUSU A., MANNERS J.M., KAZAN K. *Fusarium oxysporum* triggers tissue-specific transcriptional reprogramming in *Arabidopsis thaliana*. *PLoS ONE*, **10** (0121902), 2015.
8. AKGÜL D.S., ÖNDER S., SAVAŞ N.G., YILDIZ M., BÜLBÜL İ., ÖZARSLANDAN M. Molecular Identification and Pathogenicity of *Fusarium* Species Associated with Wood Canker, Root and Basal Rot in Turkish Grapevine Nurseries. *Journal of Fungi*, **10** (444), 2024.
9. MOHAMED R.A., AL-BEDAK O.A., HASSAN S.H.A. First record in Upper Egypt of vascular wilt on pomegranate caused by *Fusarium oxysporum*, its molecular identification and artificial pathogenicity. *Journal of Plant Disease Protection*, **128** (311), 2021.
10. SRINIVAS C., NIRMALA D.D., NARASIMHA M.K., MOHAN C.D., LAKSHMEESHA T.R., SINGH B., KALAGATUR N.K., NIRANJANA S.R., HASHEM A., ALQARAWI A.A., TABASSUM B., ABD ALLAH E.F., CHANDRA N.S. *Fusarium oxysporum* f. sp. lycopersici causal agent of vascular wilt disease of tomato: Biology to diversity- A review. *Saudi Journal of Biological Science*, **26** (7), 1315, 2019.
11. ATTIA M.S., EL-WAKIL D.A., HASHEM A.H., ABDELAZIZ A.M. Antagonistic Effect of Plant Growth-Promoting Fungi Against *Fusarium* Wilt Disease in Tomato: *In vitro* and *in vivo* Study. *Applied Biochemistry and Biotechnology*, **194** (11), 5100, 2022.
12. YOUSEF H.A., FAHMY H.M., ARAFA F.N., ABDALLAH M.Y., TAWFIK Y.M., EL HALWANY K.K., EL-ASHMANTY B.A., AL-ANANY F.S., MOHAMED M.A., BASSILY M.E. Nanotechnology in pest management: advantages, applications, and challenges. *International Journal of Tropical Insect Science*, **43** (1387), 2023.
13. ASHFAQ A., KHURSHEED N., FATIMA S., ANJUM Z., YOUNIS K. Application of nanotechnology in food packaging: pros and Cons. *Journal of Agriculture Food Research*, **7**, 2022.
14. LI Z., YU T., PAUL R., FAN J., YANG Y., WEI Q. Agricultural nanodiagnostics for plant diseases: recent advances and challenges. *Nanoscale Advances*, **2** (3083), 2020.

15. MALATHI S., PAKRUDHEEN I., KALKURA S.N., WEBSTER T.J., BALASUBRAMANIAN S. Disposable biosensors based on metal nanoparticles. *Sensors International*, **3**, **2022**.
16. NGUYEN N.N., NGUYEN N.T., NGUYEN P.T., PHAN Q.N., LE T.L., DO H.D.K. Current and emerging nanotechnology for sustainable development of agriculture: Implementation design strategy and application. *Heliyon*, **10** (10), **2024**.
17. HASIM H., RAO P., SEKHAR A., MUTHURAJU S., ASARI M., SIRAJUDEEN K. Green synthesis and characterization of silver nanoparticles using tualang honey and evaluation of their antioxidant activities. *Advances in Natural Nanoscience Nanotechnology*, **11** (2), 025010, **2020**.
18. TOLAYMAT T., BADAWY A., GENAIDY A., SCHECKEL K., LUXTON T., SUIDAN M. An evidence-based environmental perspective of manufactured silver nanoparticle in syntheses and applications: a systematic review and critical appraisal of peer-reviewed scientific papers. *Science of Total Environment*, **408** (5), 999, **2010**.
19. CHOPADE V., KAMBLE D. Application of green silver nanoparticles synthesized using leaf extract of *tridax procumbens* for preparation of clinical antimicrobial bandages. *International Journal of Pharmaceutical Investigation*, **11**(1):10, 2021.
20. WILLIAN N. Silver nanoparticles (agnps) as effective disinfectants with natural source: a new inspiration. *IOP Conference Series: Earth and Environmental Science*, **1148** (1), 012002, **2023**.
21. FARES A., MAHDY A., AHMED G. Unraveling the mysteries of silver nanoparticles: synthesis, characterization, antimicrobial effects and uptake translocation in plant-a review. *Planta*, **260** (1), 7, **2024**.
22. KHAN A.A., YAO F., CUI F., LI Y., LU L., KHAN I., JALAL A., FANG M., KHULOOD FAHAD ALABBOSH K.F., AWAD M.F., ELBOUGHDIRI N., ULLAH M.W. Comparative analysis of physicochemical properties and biological activities of crude polysaccharides isolated from selected *Auricularia cornea* strains, *Food Bioscience*, **60**, 104486, **2024**.
23. AL-ENAZI N.M., AWAAD A.S., AL-OTHMAN M.R., AL-ANAZI N.K., ALQASOUMI S.I. Isolation, identification and anti-candidal activity of filamentous fungi from Saudi Arabia soil. *Saudi Pharmaceutical Journal*, **26** (2), 253, **2018**.
24. KHAN A.A., IQBAL B., JALAL A., KHAN A.A., AL-ANDAL A., KHAN I., SUBOKTAGIN S., QAYUM A., ELBOUGHDIRI N. Advanced Molecular Approaches for Improving Crop Yield and Quality: A Review. *Journal of Plant Growth and Regulation*, **43**, 2091, **2024**.
25. SAIED E., ABDEL-MAKSoud M.A., ALFURAYDI A.A., KIANI B.H., BASSYOUNI M., AL-QABANDI O.A., BOUGAFA F.H.E., BADAWY M.S.E.M., HASHEM A.H. Endophytic *Aspergillus hirsutiae* mediated biosynthesis of silver nanoparticles and their antimicrobial and photocatalytic activities. *Frontiers in Microbiology*, **15** (1345423), **2024**.
26. SAIED E., HASHEM A.H., ALI O.M., SELIM S., ALMUHAYAWI M.S., ELBAHNASAWY M.A. Photocatalytic and Antimicrobial Activities of Biosynthesized Silver Nanoparticles Using *Cytobacillus firmus*. *Life*, **12** (1331), **2022**.
27. AL-SAHILI S.A., AL-OTIBI F., ALHARBI R.I., AMINA M., AL MUSAYEIB N.M. Silver nanoparticles improve the fungicidal properties of *Rhazya stricta* decne aqueous extract against plant pathogens. *Scientific Reports*, **14** (1), 1297, **2024**.
28. HASHEM A.H., SAIED E., AMIN B.H., ALOTIBI F.O., AL-ASKAR A.A., ARISHI A.A., ELKADY F.M., ELBAHNASAWY M.A. Antifungal Activity of Biosynthesized Silver Nanoparticles (AgNPs) against *Aspergilli* Causing *Aspergillosis*: Ultrastructure Study. *Journal of Functional Biomaterials*, **13** (242), **2022**.
29. AMIN B.H., ABOU-DOBARA M.I., DIAB M.A., GOMAA E.A., EL-MOGAZY M.A., EL-SONBATI A.Z., EL-GHAREIB M.S., HUSSEIN M.A., SALAMA H.M. Synthesis, characterization, and biological investigation of new mixed-ligand complexes. *Applied Organometallic Chemistry*, **34** (5689), **2020**.
30. ANDERSON I.C., CAMPBELL C.D., PROSSER J.I. Potential bias of fungal 18S rDNA and internal transcribed spacer polymerase chain reaction primers for estimating fungal biodiversity in soil. *Environmental Microbiology*, **5** (1), 36, **2003**.
31. BANOS S., LENTENDU G., KOPF A., TESFAYE WUBET T., FRANK OLIVER GLÖCKNER F.O., MARLIS REICH M. A comprehensive fungi-specific 18S rRNA gene sequence primer toolkit suited for diverse research issues and sequencing platforms. *BMC Microbiology*, **18** (190), **2018**.
32. PARK M.S., OH S.Y., FONG J.J., HOUBRAKEN J., LIM Y.W. The diversity and ecological roles of *Penicillium* in intertidal zones. *Scientific Reports*, **9** (13540), **2019**.
33. DEMJANOVÁ S., JEVINOVÁ P., PIPOVÁ M., REGECOVÁ I. Identification of *Penicillium verrucosum*, *Penicillium commune*, and *Penicillium crustosum* Isolated from Chicken Eggs. *Processes*, **9** (53), **2021**.
34. MOHAMMADI B., SALOUTI M. Extracellular Biosynthesis of Silver Nanoparticles by *Penicillium chrysogenum* and *Penicillium expansum*. *Synthesis and Reactivity in Inorganic, Metal-Organic, and Nano-Metal Chemistry*, **45** (6), 844, **2014**.
35. AMMAR H.A., EL-DESOUKY T.A. Green synthesis of nanosilver particles by *Aspergillus terreus* HAIN and *Penicillium expansum* HA2N and its antifungal activity against mycotoxigenic fungi. *Journal of Applied Microbiology*, **121** (1), 89, **2016**.
36. YASSIN M.A., ELGORBAN A.M., EL-SAMAWATY A.E.M.A., ALMUNQEDHI B.M.A. Biosynthesis of silver nanoparticles using *Penicillium verrucosum* and analysis of their antifungal activity. *Saudi Journal of Biological Science*, **28** (4), 2123, **2021**.
37. LIU Q., KIM Y.J., IM G.B., ZHU J., WU Y., LIU Y., BHANG S.H. Inorganic nanoparticles applied as functional therapeutics. *Advances of Functional Materials*, **31** (2008171), **2021**.
38. GUILGER-CASAGRANDE M., LIMA R. Synthesis of Silver Nanoparticles Mediated by Fungi: A Review. *Frontiers in Bioengineering and Biotechnology*, **7** (287), **2019**.
39. OSORIO-ECHAVARRÍA J., OSORIO-ECHAVARRÍA J., OSSA-OROZCO C.P., GÓMEZ-VANEGAS N.A. Synthesis of silver nanoparticles using white-rot fungus *Anamorphous Bjerkandera* sp. R1: influence of silver nitrate concentration and fungus growth time. *Scientific Reports*, **11** (1), 3842, **2011**.
40. AL-SOUB A., KHLEIFAT K., AL-TARAWNEH A., AL-LIMOUN M., ALFARRAYEH I., SARAYREH A.A., QAISI Y.A., QARALLEH H., ALQARALEH M., ALBASHAIREH A. Silver nanoparticles biosynthesis

- using an airborne fungal isolate, *Aspergillus flavus*: optimization, characterization and antibacterial activity. Iranian Journal of Microbiology, **14** (4), **2022**.
41. TANG Y., ZHAO W., ZHU G., TAN Z., HUANG L., ZHANG P., GAO L., RUI Y. Nano-Pesticides and Fertilizers: Solutions for Global Food Security. Nanomaterials (Basel), **14** (1), 90, **2023**.
  42. BADAR W., ULLAH KHAN M.A. Analytical study of biosynthesized silver nanoparticles against multi-drug resistant biofilm-forming pathogens. IET Nanobiotechnology, **14** (4), 331, **2020**.
  43. SAIED E., EID A.M., HASSAN S.E.D., SALEM S.S., RADWAN A.A., HALAWA M., SALEH F.M., SAAD H.A., SAIED E.M., FOUDA A. The catalytic activity of biosynthesized magnesium oxide nanoparticles (Mgo-nps) for inhibiting the growth of pathogenic microbes, tanning effluent treatment, and chromium ion removal. Catalysts, **11** (821), **2021**.
  44. SOLIMAN A.M., ABDEL-LATIF W., SHEHATA I.H., FOUDA A., ABDO A.M., AHMED Y.M. Green approach to overcome the resistance pattern of *Candida* spp. using biosynthesized silver nanoparticles fabricated by *Penicillium chrysogenum* F9. Biological Trace Element Research, **199** (800), **2021**.
  45. RUDRAPPA M., KUMAR R.S., NAGARAJA S.K., HIREMATH H., GUNAGAMBHIRE P.V., ALMANSOUR A.I., PERUMAL K., NAYAKA S. Myco-Nanofabrication of Silver Nanoparticles by *Penicillium brasilianum* NP5 and Their Antimicrobial, Photoprotective and Anticancer Effect on MDA-MB-231 Breast Cancer Cell Line. Antibiotics (Basel), **12** (3), 567, **2023**.
  46. BASHEER M.A., ABUTALEB K., ABED N.N., MEKAWY A.I. Mycosynthesis of silver nanoparticles using marine fungi and their antimicrobial activity against pathogenic microorganisms. Journal of Genetic Engineering and Biotechnology, **21** (127), **2023**.
  47. SUDHAKAR T., BALASHANMUGAM P., JAYAPAL P., ANISHA A., KARTHIKA D., ROSHAN S., SAKAR R. Antimicrobial activity of silver nanoparticles synthesized from *Ficus benghalensis* against human pathogens. Journal of Pharmaceutical Technology, **10** (1635), **2017**.
  48. FEMI-ADEPOJU A.G., DADA A.O., OTUN K.O., ADEPOJU A.O., FATOBA O.P. Green synthesis of silver nanoparticles using terrestrial fern (*Gleichenia Pectinata* (Willd.) C. Presl.): characterization and antimicrobial studies. Heliyon, **5** (4), **2019**.
  49. VIJAYAKUMAR G., KIM H.J., JO J.W., RANGARAJULU S.K. Macrofungal Mediated Biosynthesis of Silver Nanoparticles and Evaluation of Its Antibacterial and Wound-Healing Efficacy. International Journal of Molecular Science, **25** (2), 861, **2024**.
  50. LOTFY W.A., ALKERSH B.M., SABRY S.A., GHOZLAN H.A. Biosynthesis of Silver Nanoparticles by *Aspergillus terreus*: Characterization, Optimization, and Biological Activities. Frontiers of Bioengineering and Biotechnology, **9** (633468), **2021**.
  51. ABDELRAHIM K., MAHMOUD S.Y., MOHAMED ALI A., ALMAARY K.S., MUSTAFA A.M.A., HUSSEINY S.M. Extracellular biosynthesis of silver nanoparticles using *Rhizopus stolonifer*. Saudi Journal of Biological Science, **24** (208), **2017**.
  52. KHAN I., SIVASANKARAN N., NAGARJUNA R., GANESAN R., DUTTA J.R. Extracellular probiotic lipase capped silver nanoparticles as highly efficient broad spectrum antimicrobial agents. RSC Advances, **8** (358), **2018**.
  53. ABDELGHANY T.M., AL-RAJHI A.M.H., AL ABBOUD M.A., ALAWLAQI M.M., MAGDAH A.G., HELMY E.A.M., MABROUK A.S. Recent advances in green synthesis of silver nanoparticles and their applications: about future directions. a review. BionanoScience, **7** (1), **2017**.
  54. SOUSA F., FERREIRA D., REIS S., COSTA P. Current insights on antifungal therapy: Novel nanotechnology approaches for drug delivery systems and new drugs from natural sources. Pharmaceuticals, **13** (248), **2020**.
  55. MIKHAILOVA E.O. Silver Nanoparticles: Mechanism of Action and Probable Bio-Application. Journal of Functional Biomaterials, **11** (4), 84, **2020**.
  56. KHALIL N.M., ABD EL-GHANY M.N., RODRÍGUEZ-COUTO S. Antifungal and anti-mycotoxin efficacy of biogenic silver nanoparticles produced by *Fusarium chlamydosporum* and *Penicillium chrysogenum* at non-cytotoxic doses. Chemosphere, **218** (477), **2019**.
  57. WANG D., XUE B., WANG L., ZHANG Y., LIU L., ZHOU Y. Fungus-mediated green synthesis of nano-silver using *Aspergillus sydowii* and its antifungal/antiproliferative activities. Scientific Reports, **11** (1), **2021**.
  58. AKPINAR I., UNAL M., SAR T. Potential antifungal effects of silver nanoparticles (AgNPs) of different sizes against phytopathogenic *Fusarium oxysporum* f. sp. radicis-lycopersici (FORL) strains. SN Applied Science, **3** (506), **2021**.
  59. ANSARI M.A., KALAM A., AL-SEHEMI A.G., ALOMARY M.N., ALYAHYA S., AZIZ M.K., SRIVASTAVA S., ALGHAMDI S., AKHTAR S., ALMALKI H.D. Counteraction of biofilm formation and antimicrobial potential of *Terminalia catappa* functionalized silver nanoparticles against *Candida albicans* and multidrug-resistant Gram-negative and Gram-positive bacteria. Antibiotics, **10** (725), **2021**.
  60. MOHMED A.A., SAAD E., FOUDA A., ELGAMAL M.S., SALEM S.S. Extracellular biosynthesis of silver nanoparticles using *Aspergillus* sp. and evaluation of their antibacterial and cytotoxicity. Journal of Applied Life Science International, **11** (169), **2017**.
  61. KHAN A.A., MUHAMMAD M.J., MUHAMMAD I., JAN I., SAMIN G., ZAHID A., FOZIA, MUHAMMAD I., WANG P., LU L., FANG M., YAO F.J. Modulation of agronomic and nutritional response of *Pleurotus eryngii* strains by utilizing glycine betaine enriched cotton waste. Journal of Science, Food and Agriculture, **99** (15), 6911, **2019**.
  62. AHMAD N., NAEEM M., ALI H., KHULOOD FAHAD ALABBOSH, HAMAD HUSSAIN, ISMAIL KHAN, SHAHROOD SIDDIQUI A.S., KHAN A.A., IQBAL B. From challenges to solutions: The impact of melatonin on abiotic stress synergies in horticultural plants via redox regulation and epigenetic signaling. Scientia Horticulturae, **321**, 112369, **2023**.